Journal of Magnetic Resonance 204 (2010) 131–138

Contents lists available at ScienceDirect

Journal of Magnetic Resonance

journal homepage: www.elsevier.com/locate/jmr

# Dynamic nuclear polarization studies of redox-sensitive nitroxyl spin probes in liposomal solution

A. Milton Franklin Benial [1], Hideo Utsumi *, Kazuhiro Ichikawa, Ramachandran Murugesan [2], Ken-ichi Yamada, Yuichi Kinoshita, Tatsuya Naganuma, Masahisa Kato

*Department of Bio-functional Science, Faculty of Pharmaceutical Sciences, Kyushu University, Fukuoka 812-8582, Japan*

ARTICLE INFO

*Article history:*
Received 21 November 2009
Revised 17 February 2010
Available online 21 February 2010

*Keywords:*
OMRI
EPR
Liposome
Nitroxyl radical

ABSTRACT

Overhauser-enhanced magnetic resonance imaging (OMRI) studies of a membrane-permeable nitroxyl spin probe, $^2$H-enriched 3-methoxycarbonyl-2,2,5,5-tetramethyl-pyrrolidine-1-oxyl (MC-PROXYL), used in simultaneous molecular imaging is reported. Phantom imaging was performed with liposomal solutions of MC-PROXYL at varying spin probe and liposome concentrations using a field-cycle mode, custom-built OMRI scanner. Dynamic nuclear polarization (DNP) spectra of the liposomal solution of the spin probe, measured at 14.529 mT using a 5 mT sweep of the electron paramagnetic resonance (EPR) irradiation field showed splitting of the low and high filed hyperfine lines. Spectral measurements using $D_2O$ and a spin broadening agent, $K_3Fe(CN)_6$ confirmed that these peaks originated from water molecules in two different environments, compartmentalized with liposomes. The nuclear Overhauser enhancement measured at different EPR irradiation times and power levels showed reduction in water nuclear magnetic resonance (NMR) signal enhancement in liposomal membrane due to the reduction in the coupling constant, $\rho$. This study illustrates that OMRI can be used to differentiate between the intra- and extra- membrane water by loading the liposome vesicles with a lipid-permeable nitroxyl spin probe.


## 1. Introduction

Biological membranes are dynamic structures by virtue of the molecular rotations of the lipid chains. The molecular mobility or fluidity has decisive effects on membrane properties and functions. Liposomes with phospholipids layers are used as models for biomembranes and also as drug carriers. A wide range of amphiphilic and hydrophobic molecules can be incorporated in the liposomal membrane. Small nitroxyl spin probes are known to partition between the lipid and aqueous phases of depending on their partition coefficients [1]. This ability of spin probes makes the EPR spin probe-partition method a highly suitable technique for the investigation of membrane fluidity [2]. EPR is also used to investigate the viability of liposome as experimental drug-delivery system [3,4]. Preclinical studies using drug-encapsulated liposome have shown improvement in the sustained release of the drug, prolongation of the drug's half-life, and increase in the therapeutic index of corresponding drugs [5]. *In vivo* low frequency EPR has also been used to measure the enhancement of topical drug-delivery of hydrophilic substances [3,6]. In an earlier study we have shown that liposome can prolong the presence of the spin probe (nearly 60%) at the site of injection even up to 96 h after the injection [7]. Liposomes are also used as carriers of contrast agents by encapsulating the paramagnetic substances in vesicles [8]. The sensitivity of the liposome to breakdown under certain conditions such as at different pH or temperature can be exploited for site specific delivery, and hence for staging the imaging process.

Stable nitroxyl radicals are receiving increased attention in electron paramagnetic resonance imaging (EPRI), magnetic resonance imaging (MRI) and Overhauser-enhanced magnetic resonance imaging (OMRI) as viable reporter of *in vivo* redox status [9–15]. Simultaneous monitoring of the spin probe in aqueous and lipid phase is necessary to arrive at the redox status *in vivo* [16]. By using lipid-permeable and non-permeable nitroxyl spin probes one can monitor *intra-* or *extra*-cellular redox status. Although EPR imaging, using nitroxyl probes is capable of providing such information, OMRI has the advantage of providing co-registered images containing functional as well as anatomical information [11,14]. In addition, the MRI at 15 mT provides anatomic information with less resolution than at higher fields. By isotopically labeling nitroxyl spin probes, we have recently evaluated their dynamic nuclear polarization (DNP) properties and investigated their

* Corresponding author. Address: Department of Bio-functional Science, Faculty of Pharmaceutical Sciences, Kyushu University, Maidashi 3-1-1, Higashi-ku, Fukuoka 812-8582, Japan. Fax: +81 92 642 6626.
*E-mail address:* utsumi@pch.phar.kyushu-u.ac.jp (H. Utsumi).
[1] JSPS Postdoctoral fellow, on leave from Department of Physics, NMSSVN College, Madurai 625 019, India.
[2] School of Chemistry, Madurai Kamaraj University, Madurai 625 021, India.

1090-7807/$ - see front matter © 2010 Elsevier Inc. All rights reserved.
doi:10.1016/j.jmr.2010.02.016

application as redox-sensitive molecular probes for simultaneous molecular imaging by OMRI [14,15]. In contrast to the measurement of electron magnetization in EPR, the enhancement of proton magnetization is measured in OMRI. Therefore, OMRI has the capability to directly probe the water "status" in lipid membrane.

The relaxation of external and intra-water protons of liposomes may be modulated differently by the spin probes, leading to differential enhancement in different environments as brought by the freely or less freely-tumbling nitroxyl spin probe. NMR studies have reported that the overall relaxation behavior of paramagnetic agents-capsulated in liposome is non exponential [17]. There are two relaxation components: fast and slow, corresponding to relaxation of water protons in extra- or intra-liposomes. Such type of two compartment water model is well known in clinical MRI too. The fast relaxing water protons (transverse relaxation time ($T_2$) <1 ms) are not amenable for direct NMR imaging. Hence magnetization transfer (MT) MRI is used to probe the change in the mobility of water in certain pathological conditions [18,19]. Here we show for the first time that DNP spectra of membrane-permeable nitroxyl spin probes can be used for direct characterization of water status as "bulk" or "membrane interacting" in liposomes. By using spin broadening experiment as well as DNP studies of liposome in $D_2O$, the two peaks observed in the low-field component of the DNP spectra are confirmed to correspond to the two different water environments. It is believed that this technique will be useful to investigate the *in vivo* redox status simultaneously in aqueous and lipid phases. In addition, this technique can become a potential tool for investigating water status in biological membrane, and in viable cases can act as a complimentary tool to magnetization transfer NMR studies [18].

## 2. Methods

The spin probes, $^2$H-enriched 3-carboxy-2,2,5,5-tetramethylpyrrolidine-1-oxyl (carboxy-PROXYL) was purchased from Aldrich Chemical Co, St. Louis, MO, USA. Deuterated MC-PROXYL was synthesized as described earlier [20]. Multilamellar liposomes were prepared as follows [16]: egg phosphatidylcholine (egg PC), purchased from NOF Corporation, Japan, was first dissolved in chloroform which was later removed by rotary evaporation, yielding a thin film on the sides of a round bottom flask. The film was thoroughly dried under vacuum for about two hr. The dry lipids were suspended in spin probe containing phosphate buffer solution (PB), pH 7.4 and by vortex agitation liposome dispersions with final lipid concentration ranging from 100 to 400 mM were prepared. Nitroxyl spin probes were added to the liposomal solution and briefly sonicated. The particle size of the liposome was measured by a Zetasizer Nano light-scattering spectrophotometer (Malvern, England). The size of liposome was determined as ~100 nm, after extrusion using polycarbonate filter. These liposomal solutions containing different concentrations of MC-PROXYL and carboxy-PROXYL were used for DNP enhancement measurement and OMRI.

The DNP experiments were performed on a custom-built (Philips Research Laboratories, Hamburg, Germany), human whole-body (Magnet bore: 79 cm diameter; 125 cm length), low-field (14.529 mT) scanner, operating in a field-cycled mode [14,15]. A saddle coil (13.5 cm diameter, 23.5 cm length), tuned to 220.6 MHz was used for EPR irradiation. The NMR receive coil (solenoid of 5 cm diameter, 6 cm length) was tuned to 617 kHz with a band width of 1.5 kHz. The phantoms employed in the DNP experiments were 2 cm diameter tubes filled with 3 ml of liposomal solutions of nitroxyl spin probe of different concentrations. Following the EPR saturation pulse, a standard spin warp gradient echo sequence was initiated to obtain the OMRI images as described elsewhere [14,15]. At the beginning of the pulse sequence, a conventional (native) NMR signal (with EPR OFF) was acquired for computing the enhancement factor. A Hewlett–Packard PC (operating system, LINUX 5.2) was used for data acquisition. The images, reconstructed from the echoes by using standard software were stored in DICOM (Digital Imaging and Communications in Medicine) format. MATLAB codes were used for the computation of DNP parameters and curve fitting. Typical scan conditions were as follows: repetition time ($T_R$)/echo time ($T_E$): 2000 ms/25 ms; EPR irradiation time ($T_{EPR}$): 50–800 ms, in steps of 50 or 100 ms; EPR power, 53.8/100 W; No. of averages, 10; phase encoding steps, 64 and slice thickness, 20 mm. The image field of view (48 mm) was represented by a $64 \times 64$ matrix, with a pixel size of $0.63 \times 0.63$ mm.

Field-cycled DNP (FC-DNP) spectra of water proton in pure water as well as liposomal solution of carboxy-PROXYL and MC-PROXYL were measured at 23 °C by FC-DNP spectroscopy, by irradiating at a fixed EPR frequency (220.6 MHz) while sweeping EPR Zeeman field ($B_0^{EPR}$) from 5 to 10 mT, in steps of 0.1 mT. Near the resonances, the magnetic field was incremented in steps of 0.01 mT for better peak resolution. EPR irradiation time of 800 ms and power of 100 W were used in the experiment. EPR spectra at multiple frequencies of 0.3, 1 and 9.4 GHz were measured using a JEOL multi-frequency (electron spin resonance) ESR spectrometer (JEOL Co. Ltd., Akishima, and Tokyo, Japan). The ESR spectra were recorded using ESR spectrometers (0.3, 1 and 9.4 GHz) with 100 kHz field modulation and phase sensitive detection. The ESR spectrometers with frequency 0.3, 1 and 9.4 GHz were operated with microwave power 100, 10 and 5 mW, respectively. The reproducibility of data was confirmed with repeated experiments. The fitted parameters were also shown good correlation ($R^2 > 0.999$).

## 3. Results and discussion

### 3.1. DNP spectra

FC-DNP spectra of liposomes with nitroxyl radicals were collected with a field sweep of 5 mT using a field-cycled DNP pulse sequence as described previously [14,15]. When an EPR resonance is encountered, the NMR signal amplitude is altered due to the Overhauser effect. Therefore, a plot of NMR signal amplitude versus $B_0^{EPR}$ shows the positions of the EPR resonances. The relative amplitudes of the peaks (or, more usually troughs) provide information on the EPR line intensities, modulated by the electron–proton coupling. The DNP spectra of the spin probes, given in Fig. 1 show three hyperfine lines for $^{14}$N. The position of the peaks and the full-width at half-maximum (FWHM) of each line are listed in Table 1. Second–order effects in hyperfine splitting and a small nuclear spin quantum number ($m_I$) dependent line width were observed.

A comparative account of the DNP spectra with the EPR spectra may provide better understanding of the origin of the various peaks. Hence multi-frequency EPR spectra of the spin probes in liposome dispersions were measured and these are shown in Fig. 2. No noticeable change was observed between the DNP spectra of carboxy-PROXYL in pure water and liposomal solution. However, due to its relatively large hydrophobic nature (partition coefficients of carboxy-PROXYL and MC-PROXYL in octanol–water system are 0.02 and 8.7, respectively [16], the spin probe MC-PROXYL partitions between the lipid phase and water, and the resulting EPR spectrum consists of two distinct triplets, one arising from the spin probe in water phase and the other, resulting from the spin probe molecules in the hydrophobic environment, provided by the interior of the phospholipids bilayer. Thus each spectrum is a superposition of two spectra. Small differences in the isotropic hyperfine coupling constants and $g$ factors for the

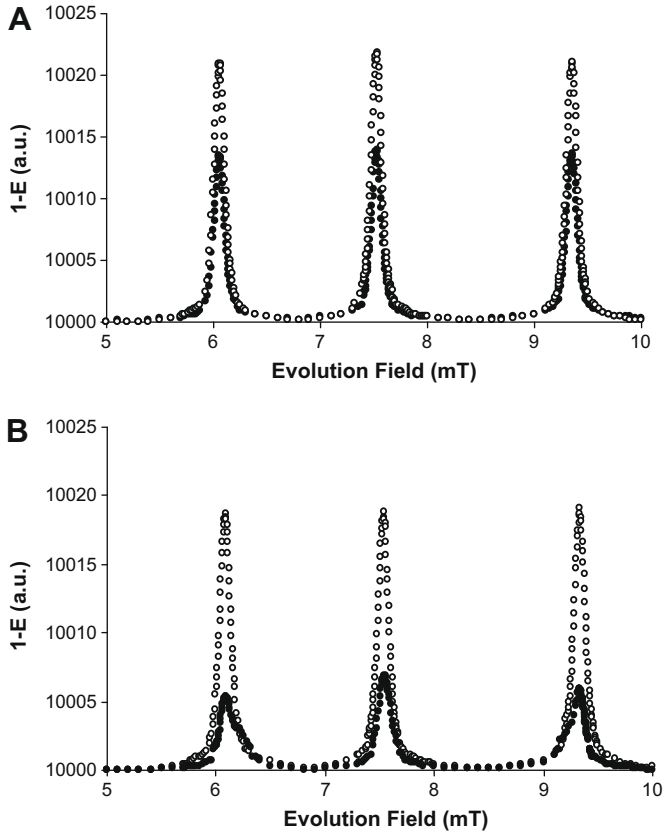


**Fig. 1.** FC-DNP spectra of 2 mM solutions of carboxy-PROXYL (A) and MC-PROXYL (B) in water (○) and liposome (●). Pulse sequence parameters: TR/$T_{ESR}$/TE, 2000/800/25 ms; No. of averages, 2; power, 100 W; other scan parameters are as given under Section 2.

spin-label in each environment result in a partial resolution of the high-field hyperfine line at X-band. However, both the L-band as well as the 300 MHz spectra showed well resolved low-field lines.

The expanded low-field line of the proton DNP spectra of proton, given in Fig. 3 clearly reflects a similar behavior. A peak and a shoulder can be readily noticed, suggesting that there are two different environments of water molecule. The separation of the peaks indicates that the DNP is maintained and the exchange of water between the two respective environments is slow in NMR time scale. The spin-label exchange between the two environments is also likely to affect the peak separation. The relative intensities of the two peaks were found to depend upon liposome and spin probe concentrations. For example, Fig. 4 shows OMRI images of 2 mM MC-PROXYL in different liposome concentrations. These images were obtained by irradiating the EPR resonance at 6.20 mT which is the resonance field of lipidic nitroxyl signal. With increase in liposome concentration, it is likely that the intra-lipid quantity of MC-PROXYL increases, leading to an increase in the signal enhancement. This is very clearly illustrated in the phantom imaging results of liposomes given in Fig. 5. By leaving the tubes containing the liposomal solution in an inert atmosphere for seven days, the liposome phase got separated and settled at the bottom of the tube as seen in the photographs (Fig. 5). In the OMRI images, the area corresponding to the liposomal region shows increase in intensity with increase in liposome concentration. The slightly increased intensity of the lipid phase in 400 mM liposome dispersions compared to the 200 mM dispersions shows the presence of larger amount of intra-lipid quantity of MC-PROXYL in 400 mM dispersion, which leads to the increase in the signal enhancement. Similarly, OMRI image was obtained by saturating the resonance at 6.09 mT shows high intensity in 200 mM liposome dispersions compared to the 400 mM liposome dispersions, which shows the presence of larger amount of bulk water in 200 mM liposome dispersions, exhibiting a close match with the photograph.

In aqueous phase, water molecules have direct access to a more labile nitroxyl agent, and relaxation occurs through a magnetic dipolar interaction between the water protons and paramagnetic spin probes. In native MRI, the spectral densities of the fluctuating $^1H$–$^1H$ dipolar fields, modulated by random molecular motion determine the proton spin–lattice relaxation time ($T_1$) and $T_2$ contrasts. But, in OMRI, the spectral density function of the electron–proton interaction plays a major role. The enhancement is appreciable only when molecular motion takes place in a time scale faster than the inverse Larmor frequency of the electron spin. In the extreme narrowing limit, the inverse electronic Larmor frequency is larger than the characteristic correlation time of the molecular motion, leading to larger enhancement in aqueous phase.

It is important to ascertain that we are in fact monitoring the protons of water molecules in two different environments, and not protons of other origin such as the phosphate lipid. Hence we measured DNP spectra of the spin probes in liposomal solutions prepared using $D_2O$. As seen in Fig. 3, under such conditions, no resonances were observed. To observe the resonance from the quadrupolar $^2H$ nucleus, the irradiation frequency should be reduced by a factor of about 6.51. Such an excitation source is not available in our instrument and hence we were unable to carry out $^2H$-irradiation. Nevertheless, this experiment supports the argument that both the peaks originate from the proton resonance of $H_2O$. We further resorted to spin broadening study to separate the lipid phase proton signal from the large aqueous phase signal. $K_3Fe(CN)_6$ has been used as a spin broadening agent to monitor the intracellular viscosity by EPR spin-labeling technique [21]. $K_3Fe(CN)_6$ does not penetrate the cells, and at 80 mM concentration it completely broadens external aqueous component signal of the spin-label. Fig. 6 shows the DNP spectra of 2 mM MC-PROXYL in 400 mM liposome dispersions in $H_2O$, after adding exogenous 80 mM $K_3Fe(CN)_6$. It is readily seen that the extra-vesicular water–proton signal from the aqueous phase is almost completely lost. The paramagnetic agent broadens the spin probe signal outside the liposomes which makes saturation of the EPR line very difficult, resulting in the loss of enhancement. However, the paramagnetic

**Table 1**
Peak positions and FWHM of DNP spectra of 2 mM MC-PROXYL in water and liposome dispersion.

| MC-PROXYL | Peak position (mT) | | | FWHM (μT) | | | $E_{max}$ |
|---|---|---|---|---|---|---|---|
| | Low frequency | Middle frequency | High frequency | Low frequency | Middle frequency | High frequency | |
| Water | 6.09 | 7.54 | 9.34 | 115 | 125 | 120 | −63.7 |
| Liposome aqueous phase | 6.09 | 7.55 | 9.34 | 120 | 135 | 130 | −30.4 |
| Lipid phase | 6.22 | – | 9.22 | 145 | – | 140 | −14.8 |

$E_{max}$ is the extrapolated enhancement factor at complete saturation measured for 2 mM concentration.
— Indicates that the spectral line corresponds to lipid phase is not resolved at the middle frequency.

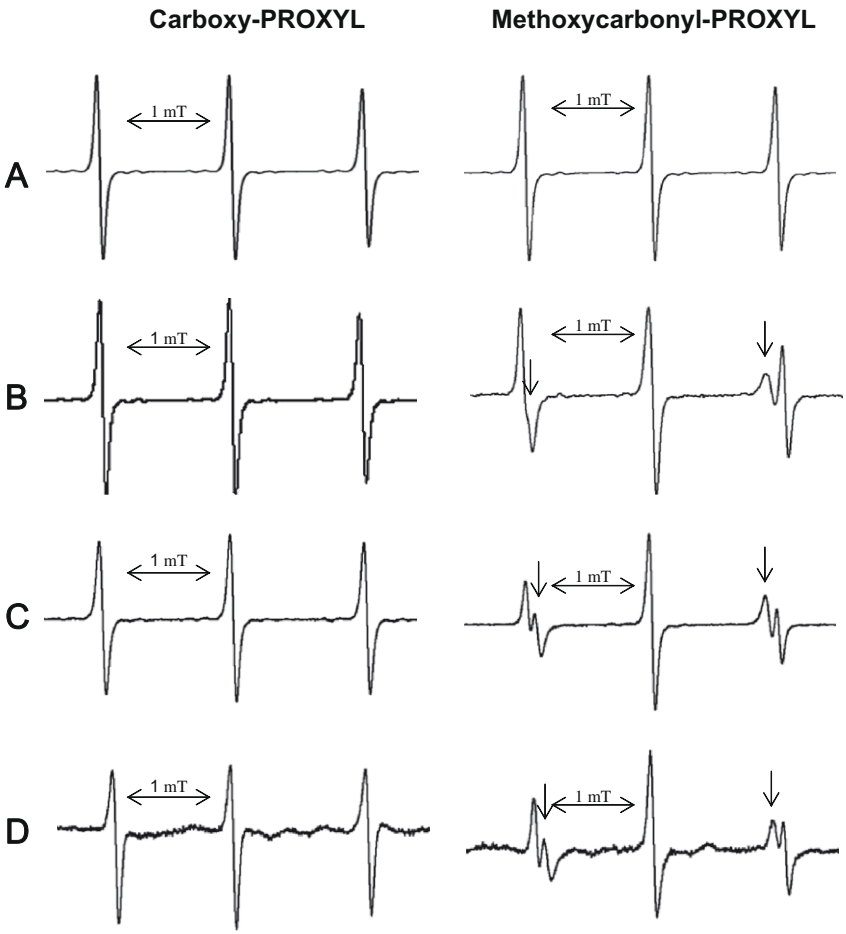


**Fig. 2.** EPR spectra of 2 mM carboxy-PROXYL and MC-PROXYL (A) in water at X-band and (B–D) in 400 mM liposome at 9.4 GHz, 1 GHz and 300 MHz, respectively. The arrows indicate the lipidic component.

agent, $K_3Fe(CN)_6$ is not able to penetrate the lipid membrane, and hence the spin probe spectrum inside the lipid phase is not broadened. Therefore, during DNP experiment, only the spectral line at 6.20 mT is saturated, and thus enhancement of NMR signal from protons of the intra-lipid aqueous environment alone is observed.

### 3.2. Enhancement factor

The enhancement, $E$ of the NMR signal of the $^1$H nuclei of water molecules with couplings to an unpaired electron spin, electron spin quantum number ($S$) = 1/2 of the dissolved spin probe, is given by

$$E = \frac{\langle I_Z \rangle}{I_0} = 1 - \rho f_s \frac{|\gamma_e|}{\gamma_N}, \quad (1)$$

Here $\langle I_z \rangle$ denotes the expectation value of the dynamic nuclear polarization, $I_0$ is its thermal equilibrium value, $\rho$ is the coupling parameter, $f$ is the leakage factor, $s$ denotes the saturation parameter, and $\gamma_e$ and $\gamma_N$ are, respectively, the electron and nuclear gyromagnetic ratios. Complete saturation of one of the EPR lines requires very high EPR irradiation power. The saturation parameter, $s$ can be determined, for a given concentration by measuring the enhancement as a function of applied EPR irradiation power. The intercept of a plot of $1/(1-E)$ against $1/P$ can be used to estimate $E_{max}$, the enhancement factor at complete EPR saturation. $E_{max}$, also known as the ultimate enhancement factor, characterizes the overall interaction of the spin probe with the solvent water molecules. In addition, $E_{max}$ enables to compare the enhancement efficiency of nitroxyl agents at different environments without being biased by instrumental parameters such as resonator Q-factor, EPR power, $T_{EPR}$, etc. Therefore, enhancements at various power levels were measured for 2 mM aqueous solutions of MC-PROXYL. These results, plotted in Fig. 7 as reciprocal enhancement $1/(1-E)$, against reciprocal power, $1/P$, show a linear relation. On extrapolation to $1/P = 0$, the $E_{max}$ values were computed and these values are included in Table 1. For this investigation, EPR power level up to 152.8 W was used to make the extrapolation more accurate. The NMR signal enhancement is considerably affected by the proton mobility. Reduction in coupling constant ($\rho$) is observed with decrease in mobility [22,23]. This may be the origin for the observed order of $E_{max}$, pure water > bulk water in liposomes > water interacting with lipid bilayer.

### 3.3. $T_1$ of water protons in the two environments

Another factor that affects the build up and decays of the polarization of water protons is the leakage factor that is related to $T_1$ by

$$f = 1 - (T_1/T_{10}) \quad (2)$$

Here $1/T_{10}$ denotes the intrinsic nuclear relaxation rate of the protons of the solvent water molecules in the absence of nitroxyl agent. Hence it would be of interest to measure $T_1$ in the two different environments. $T_1$ values at the very low Zeeman field (14.529 mT) used in OMRI can be obtained by fitting the enhancement factors as a function of $T_{ESR}$ using the equation [24].

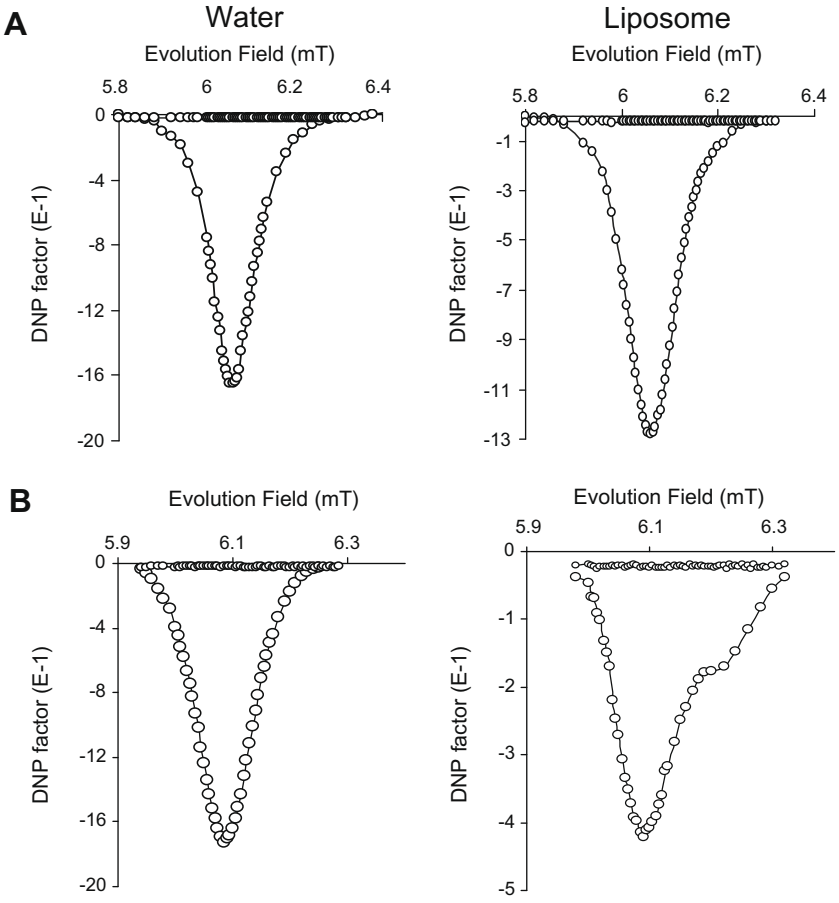


**Fig. 3.** DNP spectra (expanded low-field resonance line) of 2 mM (A) carboxy-PROXYL and (B) MC-PROXYL in water and 400 mM liposome. Horizontal lines correspond to the measurements where $H_2O$ was replaced by $D_2O$ and these lines indicate that there is no enhancement in $D_2O$. Pulse sequence parameters: TR/$T_{ESR}$/TE, 2000/800/25 ms; No. of averages, 2; power, 100 W; other scan parameters are as given under Section 2.

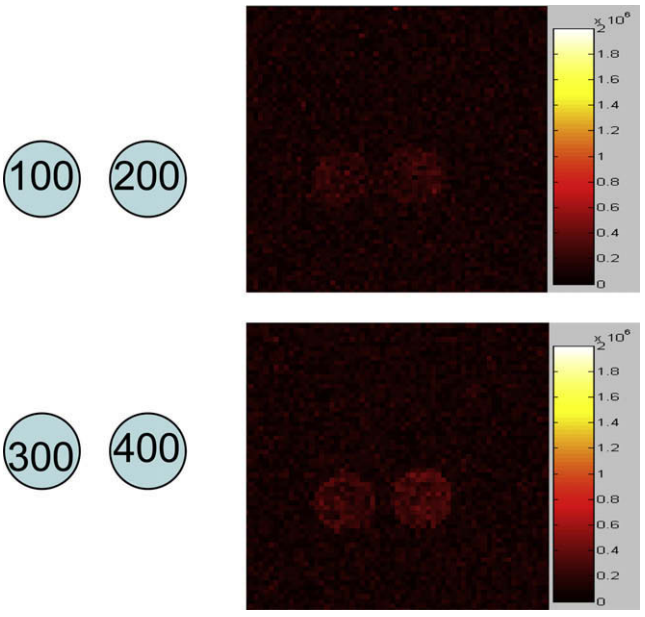


**Fig. 4.** Phantom images of 2 mM MC-PROXYL, obtained by irradiating the EPR resonance at 6.20 mT in 100, 200, 300 and 400 mM liposome. Pulse sequence parameters: TR/$T_{ESR}$/TE, 2000 ms/800 ms/25 ms; No. of averages, 2, power = 100 W; other scan parameters are as given under Section 2.

$$E - 1 = (E_{inf} - 1) \times \left(1 - \exp^{-\frac{T_{ESR}}{T_1}}\right) \quad (3)$$

Here, $E$ is the Overhauser enhancement factor, and $E_{inf}$ is the theoretical maximum enhancement factor corrected for the actual $T_1$. Hence DNP enhancement was measured as a function of $T_{ESR}$ for 2 mM MC-PROXYL and these results are presented in Fig. 8. By curve fitting the observed enhancement factors to equation [3], the NMR spin–lattice relaxation times were computed for the intra- and extra-lipid phases. These values are given in Table 2. The observed small difference between the $T_1$ values of bulk water and water interacting with lipid bilayer of 2 mM nitroxyl probe rules out any significant contribution from the leakage factor. Another factor that critically affects the enhancement is the saturation of the degree of the electron spin, given by

$$S = [S_0 - \langle S_z \rangle]/S_0 \quad (4)$$

at a given EPR power depends on the electron spin relaxation rates of the nitroxyl agent. The small increase in line width in lipid phase (Table 1) or reduced mobility of water may contribute to the reduced enhancement observed in the lipid phase.

Liposome is a promising carrier system for diagnostic agents for use in single-photon emission computed tomography (SPECT) or magnetic resonance imaging (MRI), as well as for therapeutic agents to treat diseases such as cancer. Phospholipids vesicles have been observed to accumulate in implanted tumors of mice [25]. NMR studies are used to investigate the water diffusion in lipid layers [26,27]. There is also increasing interest in clinical MRI to understand the status of water, because the mobility of water is different in different pathological conditions. But, the signal obtained in clinical MRI comes mainly from mobile proton. These are largely present in free water with a smaller contribution from

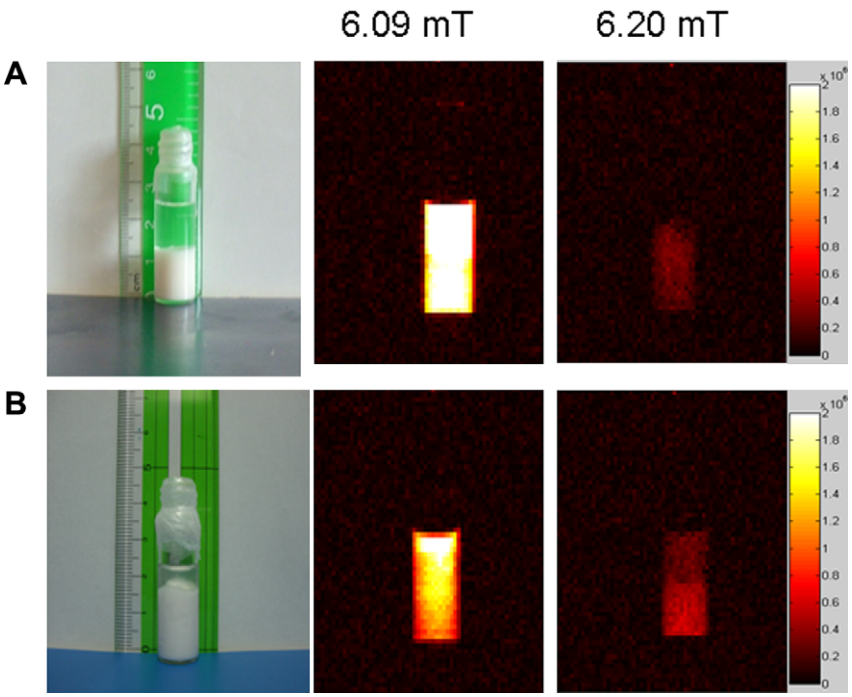


**Fig. 5.** Phantom images ($B_0^{EPR}$ at 6.09 and 6.20 mT) of 2 mM MC-PROXYL recorded 7 days after the preparation of (A) 200 mM and (B) 400 mM liposome dispersions. Pulse sequence parameters: TR/$T_{ESR}$/TE, 2000 ms/800 ms/25 ms; No. of averages, 2; power, 100 W; other scan parameters are as given under Section 2. The photographs of phantoms (A) and (B), also taken after 7 days of sample preparation show that the liposome layer is settled at the bottom of the tube.

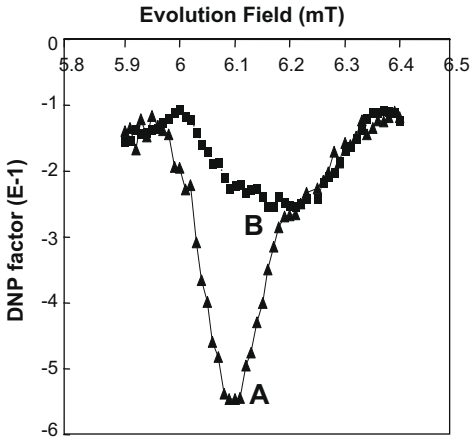


**Fig. 6.** DNP spectra of $^2$H-enriched 2 mM MC-PROXYL in 400 mM liposomal solution, (A) in the absence and (B) in the presence of 80 mM $K_3Fe(CN)_6$. Pulse sequence parameters: TR/$T_{ESR}$/TE, 2000/800/25 ms; No. of averages, 2; power, 100 W; other scan parameters are as given under Section 2.

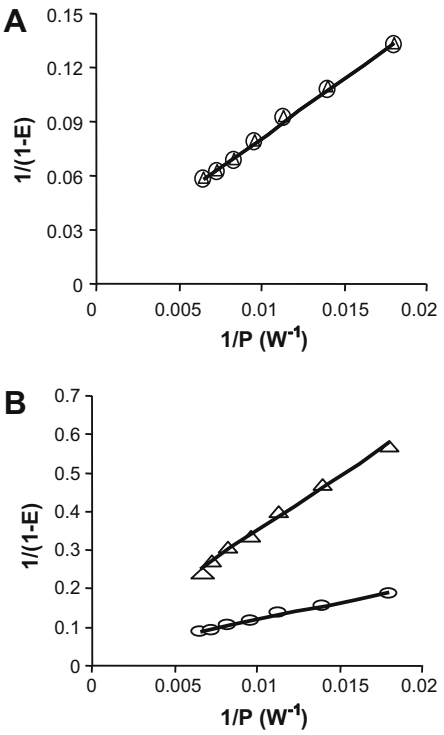


**Fig. 7.** Effect of EPR irradiation power on the enhancement (A) for 2 mM carboxy-PROXYL (○) and MC-PROXYL (△) in water. (B) Enhancement for 2 mM MC-PROXYL in 400 mM liposome at $B_0^{EPR}$ = 6.09 (△ intra-lipid water) and 6.20 mT (○ extra-lipid water). The EPR power varied from 53.8–152.8 W. EPR irradiation time, 800 ms; other scan parameters are as given in the Section 2.

lipid. There are, in addition, a large number of protons in tissues contained in macromolecules or in water bound to these macromolecules. No signal is normally detected from these protons by standard clinical imaging techniques, because they have a very short $T_2$ value (of the order of 1 ms or less) and any transverse magnetization is rapidly dephased before data collection is possible. However, the bound pool influences the signal obtained from the free pool even though the bound pool cannot be directly visualized. In MT imaging, the normal equilibrium between free and bound pools is perturbed and the resulting contrast, referred to as magnetization transfer contrast and indicates the exchange processes with the bound pool in that particular tissue.

Nitroxyl agents find wide application as useful probes for investigating inhomogeneous systems, such as membranes, in which two or more regions of different solvent characteristics (e.g., hydrophobic and hydrophilic) are present [28,29]. The application is based on the solvent dependence of EPR parameters of the probe,

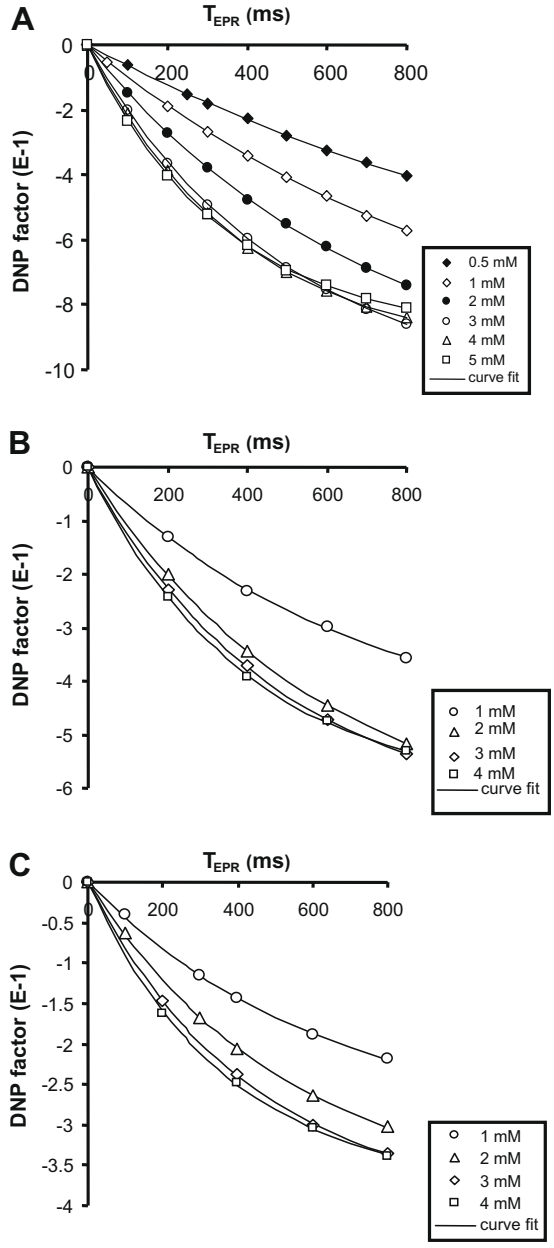


**Fig. 8.** The effect of $T_{EPR}$ on the DNP enhancement of protons dispersions for various concentrations of MC-PROXYL in (A) pure water (EPR power, 53.8 W) (B) extra-lipid and (C) intra-lipid phase in 400 mM liposome dispersion (EPR power, 100 W); other scan parameters are as given in the Section 2.

**Table 2**
Spin lattice relaxation time of water proton $T_1$ (ms) for MC-PROXYL in pure water and in liposome.

| Spin probe concentration (mM) | Water | Liposomal solution | |
|---|---|---|---|
| | | Aqueous phase | Lipid phase |
| 1 | 1040 | 679 | 642 |
| 2 | 696 | 577 | 546 |
| 3 | 481 | 472 | 439 |
| 4 | 388 | 395 | 370 |

and the possibility then exists of using the label to probe properties of each component of an inhomogeneous system. This ability of nitroxyl probes to partition between a membrane phase and the surrounding aqueous medium and the difference in hyperfine constants of nitroxyl probe in the two environments are very well used for investigating lateral phase separation in lipids [1]. Nevertheless, the information about the water status in the two different phases cannot be directly obtained by the EPR method. In contrast to EPR, OMRI measures directly the enhancement of proton magnetization, thereby providing the capability to directly probe the water status in lipid membrane. In addition, the possibility of monitoring the two phases simultaneously in OMRI opens up a way to look at the loss of spin count in both the phases. This will enable investigation of redox status in the two different environments. Therefore, the measurement of DNP parameters that govern the water–proton signal enhancement in lipid membranes can provide guidelines for further enhancing the utility of OMRI for investigating the redox status simultaneously in two different environments.

## 4. Conclusions

We have measured Overhauser enhancement over a wide range of concentration, saturating EPR power level and EPR irradiation time completely to compare the various DNP properties of the spin probes in intra-lipid and extra-lipid environments. It is demonstrated that OMRI, with the use of a lipid partitioning spin probe can be a very useful technique for the study of properties of the intracellular aqueous compartments of biological systems. FC-DNP spectra reported here demonstrate the presence of two distinct water protons corresponding to intra- and extra-lipid water molecules, making it possible to directly probe the "bulk" and "lipid interacting" water molecules. Our purpose here was to show the feasibility of this type of study. It appears that OMRI can be very helpful in providing such information. One of the advantages of this technique is that it may provide a more direct measure of the bound water pool, independent on model-based fitting procedures which are necessary in the computation and interpretation of relaxation rates in magnetization transfer MRI. The difficulties involved in utilizing this technique include: overlap of spectra from the label in different environments, leading to uncertainties in the OMRI parameters. Better probes for this purpose should have large partition coefficient and at the same time small line width even in less mobile condition. We envisage also that by designing viscosity-prone spin probes one can use this technique to investigate intracellular viscosity.

## Acknowledgments

This work was supported by the Grant-in-Aid for Scientific Research (A) from JSPS (Japan Society for the Promotion of Science), and for Scientific Research on Priority Areas "Application of Molecular Spins" from the Ministry of Education, Culture, Sports, Science and Technology of Japan, and by 21st Century Centers of Excellence (COE) program of Kyushu University from the Ministry of Education, Culture, Sports, Science and Technology of Japan. This work was supported by "Development of System and Technology for Advanced Measurement and Analysis", Japan Science and Technology Agency. This work was also supported by the Grant-in-Aid for JSPS Postdoctoral Fellowship for Foreign Researchers (ID No. P 04489). One of the authors (A. Milton Franklin Benial) thanks NMSSVN College, Madurai 625 019, and India for encouragement and leave for postdoctoral research studies.

## References

[1] E.J. Shimshick, H.M. McConnell, Lateral phase separation in phospholipid membranes, Biochemistry 12 (1973) 2351–2360.
[2] K. Vrhovnik, J. Kristl, M. Sentjurc, J. Smid-Korbar, Influence of liposome bilayer fluidity on the transport of encapsulated substance into the skin as evaluated by EPR, Pharm. Res. 15 (1998) 525–530.

[3] T. Yamaguchi, S. Itai, H. Hayashi, S. Soda, A. Hamada, H. Utsumi, In vivo ESR studies on pharmacokinetics and metabolism of parenteral lipid emulsion in living mice, Pharm. Res. 13 (5) (1996) 729–733.
[4] K. Matsumoto, K. Yahiro, K. Yamada, H. Utsumi, In vivo EPR spectroscopic imaging for a liposomal drug delivery system, Magn. Reson. Med. 53 (2005) 1158–1165.
[5] A. Gabizon, D. Goren, A.T. Horowitz, D. Tzemech, A. Lossos, T. Siegal, Long-circulating liposomes for drug delivery in cancer therapy: a review of biodistribution studies in tumor-bearing animals, Adv. Drug Deliv. Rev. 24 (1997) 337–344.
[6] L. Honzak, M. Sentjurc, H.M. Swartz, In vivo EPR of topical delivery of a hydrophilic substance encapsulated in multilamellar liposomes applied to the skin of hairless and normal mice, J. Control. Release 66 (2000) 221–228.
[7] K.P. Moll, R. Stößer, W. Herrmann, H. Borchert, H. Utsumi, In vivo EPR studies on subcutaneously injected multilamellar liposomes in living mice, Pharm. Res. 21 (2004) 2017–2024.
[8] V. Weissig, J. Babich, V. Torchilin, Long-circulating gadolinium-loaded liposomes: potential use for magnetic resonance imaging of the blood pool, Colloids Surf. B Biointerfaces 18 (2000) 293–299.
[9] D. Grucker, T. Guiberteau, B. Eclancher, J. Chambron, R. Chiarelli, A. Rassat, G. Subra, B. Gallez, Dynamic nuclear-polarization with nitroxyls dissolved in biological-fluids, J. Magn. Reson. 106 (1995) 101–109.
[10] K. Golman, J.S. Petersson, J.H. Ardenkjaer-Larsen, I. Leunbach, L.G. Wistrand, G. Ehnholm, K. Liu, Dynamic in vivo oxymetry using overhauser enhanced MR imaging, J. Magn. Reson. Imaging 12 (2000) 929–938.
[11] M.C. Krishna, S. English, K. Yamada, J. Yoo, R. Murugesan, N. Devasahayam, J.A. Cook, K. Golman, J.H. Ardenkjaer-Larsen, S. Subramanian, J.B. Mitchell, Overhauser enhanced magnetic resonance imaging for tumor oximetry: coregistration of tumor anatomy and tissue oxygen concentration, Proc. Natl. Acad. Sci. USA 99 (2002) 2216–2221.
[12] R. Murugesan, S. English, K. Reijnders, K. Yamada, J.A. Cook, J.B. Mitchell, S. Subramanian, M.C. Krishna, Fluorine electron double resonance imaging for $^{19}F$ MRI in low magnetic fields, Magn. Reson. Med. 48 (2002) 523–529.
[13] H. Li, Y. Deng, G. He, P. Kuppusamy, D.J. Lurie, J.L. Zweier, Proton electron double resonance imaging of the in vivo distribution and clearance of a triaryl methyl radical in mice, Magn. Reson. Med. 48 (2002) 530–534.
[14] H. Utsumi, K. Yamada, K. Ichikawa, K. Sakai, Y. Kinoshita, S. Matsumoto, M. Nagai, Simultaneous molecular imaging of redox reactions monitored by Overhauser-enhanced MRI with 14 N- and 15 N-labeled nitroxyl radicals, Proc. Natl. Acad. Sci. USA 103 (2006) 1463–1468.
[15] A.M.F. Benial, K. Ichikawa, R. Murugesan, K. Yamada, H. Utsumi, Dynamic nuclear polarization properties of nitroxyl radicals used in Overhauser-enhanced MRI for simultaneous molecular imaging, J. Magn. Reson. 182 (2006) 273–282.
[16] M. Yamato, T. Egashira, H. Utsumi, Application of in vivo ESR spectroscopy to measurement of cerebrovascular ROS generation in stroke, Free Radic. Biol. Med. 35 (12) (2003) 1619–1631.
[17] G. Bacic, M.R. Niesman, H.F. Bennett, R.L. Magin, H.M. Swartz, Modulation of water proton relaxation rates by liposomes containing paramagnetic materials, Magn. Reson. Med. 6 (1988) 445–458.
[18] D. Tozer, A. Ramani, G.J. Barker, G.R. Davies, D.H. Miller, P.S. Tofts, Quantitative magnetization transfer mapping of bound protons in multiple sclerosis, Magn. Reson. Med. 50 (2003) 83–91.
[19] J.G. Sled, G.B. Pike, Quantitative imaging of magnetization transfer exchange and relaxation properties in vivo using MRI, Magn. Reson. Med. 46 (2001) 923–931.
[20] H. Sano, K. Matsumoto, H. Utsumi, Synthesis and imaging of blood–brain-barrier permeable nitroxyl-probes for free radical reactions in brain of living mice, Biochem. Mol. Biol. Int. 42 (1997) 641–647.
[21] P.D. Morse, Use of the spin label tempamine for measuring the internal viscosity of red blood cells, Biochem. Biophys. Res. Commun. 77 (1997) 1486–1491.
[22] I. Nicholson, D.J. Lurie, F.J.L. Robb, The application of proton–electron double-resonance imaging techniques to proton mobility studies, J. Magn. Reson. B 104 (1994) 250–255.
[23] P.L. de Sousa, R.E. de Souza, M. Engelsberg, L.A. Colnago, Mobility and free radical concentration effects in proton–electron double-resonance imaging, J. Magn. Reson. 135 (1998) 118–125.
[24] S. Matsumoto, H. Utsumi, T. Aravalluvan, K. Matsumoto, A. Matsumoto, N. Devasahayam, A.L. Sowers, J.B. Mitchell, S. Subramanian, M.C. Krishna, Influence of proton $T_1$ on oxymetry using Overhauser-enhanced magnetic resonance imaging, Magn. Reson. Med. 54 (2005) 213–217.
[25] R.T. Proffitt, L.E. Williams, C.A. Presant, G.W. Tin, J.A. Uliana, R.C. Gamble, J.D. Baldeschwieler, Liposomal blockade of the reticuloendothelial system: improved tumor imaging with small unilamella vesicles, Science 220 (1983) 502–505.
[26] J. Andrasko, S. Forsen, NMR study of rapid water diffusion across lipid bilayers in dipalmitoyl lecithin vesicles, Biochem. Biophys. Res. Commun. 60 (1974) 813–819.
[27] D. Huster, A.J. Jin, K. Arnold, K. Gawrisch, Water Permeability of polyunsaturated lipid membranes measured by $^{17}0$ NMR, Biophys. J. 73 (1997) 855–864.
[28] B.P. Soule, F. Hyodo, K. Matsumoto, N.L. Simone, J.A. Cook, M.C. Krishna, J.B. Mitchell, The chemistry and biology of nitroxide compounds, Free Radic. Biol. Med. 42 (2007) 1632–1650.
[29] T. Tsutsumi, T. Ide, M. Yamato, W. Kudou, M. Andou, Y. Hirooka, H. Utsumi, H. Tsutsui, K. Sunagawa, Modulation of the myocardial redox state by vegal nerve stimulation after experimental myocardial infarction, Cardiovas. Res. 77 (2008) 713–721.